

Diagnostic Analysis of the Evolution Mechanism for a Vortex over the Tibetan Plateau in June 2008

LI Lun^{1,3} (李论), ZHANG Renhe^{*2} (张人禾), and WEN Min² (温敏)

¹*State Key Laboratory of Numerical Modeling for Atmospheric Sciences and Geophysical Fluid Dynamics,
Institute of Atmospheric Physics, Chinese Academy of Sciences, Beijing 100029*

²*State Key Laboratory of Severe Weather, Chinese Academy
of Meteorological Sciences, Beijing 100081*

³*Graduate University of the Chinese Academy of Sciences, Beijing 100049*

(Received 11 May 2010; revised 2 August 2010)

ABSTRACT

Based on the final analyses data (FNL) of the Global Forecasting System of the NCEP and the observational radiosonde data, the evolution mechanism of an eastward-moving low-level vortex over the Tibetan Plateau in June 2008 was analyzed. The results show that the formation of the vortex was related to the convergence between the northwesterly over the central Tibetan Plateau from the westerly zone and the southerly from the Bay of Bengal at 500 hPa, and also to the divergence associated with the entrance region of the upper westerly jet at 200 hPa. Their dynamic effects were favorable for ascending motion and forming the vortex over the Tibetan Plateau. Furthermore, the effect of the atmospheric heat source (Q_1) is discussed based on a transformed potential vorticity (PV) tendency equation. By calculating the PV budgets, we showed that Q_1 had a great influence on the intensity and moving direction of the vortex. In the developing stage of the vortex, the heating of the vertically integrated Q_1 was centered to the east of the vortex center at 500 hPa, increasing PV tendency to the east of the vortex. As a result, the vortex strengthened and moved eastward through the vertically uneven distribution of Q_1 . In the decaying stage, the horizontally uneven heating of Q_1 at 500 hPa weakened the vortex through causing the vortex tubes around the vortex to slant and redistributing the vertical vorticity field.

Key words: Tibetan Plateau low-level vortex, atmospheric heat source, PV tendency equation

Citation: Li, L., R. H. Zhang, and M. Wen, 2011: Diagnostic analysis of the evolution mechanism for a vortex over the Tibetan Plateau in June 2008. *Adv. Atmos. Sci.*, **28**(4), 797–808, doi: 10.1007/s00376-010-0027-y.

1. Introduction

The low-level vortex formed over the Tibetan Plateau in boreal summer is the major rain-producing system over the Tibetan Plateau. Most of the vortices originate over the central-western plateau, move eastward, and decay over the eastern plateau. Some of them may move eastward off the plateau and trigger precipitation to the east of the Tibetan Plateau, giving rise to disastrous weather events such as rainstorms and thunderstorms over eastern China (Ye and Gao, 1979; Qiao and Zhang, 1994; Li, 2002). The region

with the highest occurrence frequency of the vortices is around Naqu (32°N, 92°E), and the highest disappearance frequency is near Ganzi (32°N, 100°E) (Lhasa group for Tibetan Plateau meteorology research, 1981; Luo, 1992). Most vortices have an eye structure with a warm core, which is similar to the structure of typhoon (Qiao and Zhang, 1994; Li and Liu, 2006). The typical horizontal and vertical scale of a plateau vortex is about 500 km and 2–3 km respectively. Its cyclonic circulation is primarily confined to the lower-middle troposphere, with positive vorticity disappearing above 400 hPa and the water vapor mainly con-

* Corresponding author: ZHANG Renhe, renhe@cams.cma.gov.cn

centrating below 500 hPa (Lhasa group for Tibetan Plateau meteorology research, 1981; Luo, 1992; Luo et al., 1993).

Much research has been done on the evolution mechanism of the Tibetan Plateau low-level vortices. Previous studies pointed out that the divergence in the upper troposphere was the major factor accounting for the eastward movement of the plateau vortices (Liu and Fu, 1985), and their movement direction and speed depended on the air stream above the vortices at 300–200 hPa (Qiao, 1987). It was suggested that the condensation latent heat release was a major factor in the development process, and the intensity of the vortex had a close relationship with the altitude of the plateau. The elevated terrain appeared to enhance the influence of thermodynamic processes (Dell'Osso and Chen, 1986; Shen et al., 1986a; Wang, 1987). Some previous synoptic studies also inferred that the sensible heating made a positive contribution to the vortex (Lhasa group for Tibetan Plateau meteorology research, 1981), but no direct proof was given, and they only focused on the effect of sensible heating itself by using a numerical experiment on one case (Shen et al., 1986b) and solving a linearized vortex equation (Li and Zhao, 2002). Ding and Lu (1990) used a five-layer primitive equation model to simulate the eastward movement of a vortex over the Tibetan Plateau. They claimed that diabatic factors such as radiation and large-scale condensation latent heat might only affect the intensity of the vortex. Luo et al. (1991) analyzed a case of the plateau vortices and found that the genesis and development of the plateau vortex were closely interrelated with the variations of the atmospheric heat field. The strengthening and weakening of the vortex were related to variations of the atmospheric heat field. Chen et al. (1996) simulated three vortex cases and found that their disappearances in the sloping terrain over the eastern Tibetan Plateau were associated with the weakening of the surface heating.

The previous studies have analyzed features of the large-scale circulation and the energy budget associated with the plateau vortex, emphasizing the effect of the atmospheric heat source on the intensity of the plateau vortex. However, can the atmospheric heat source also affect the eastward motion of the vortex, and how? In order to further understanding of the physical mechanisms underlying eastward movement, a vortex case in June 2008 was selected for this study. In section 2 we describe the data and method. The role of the large-scale circulation in the vortex genesis process is analyzed in section 3. In section 4 we discuss the effect of the atmospheric heat source on the vortex's trajectory and intensity through diagnosing the potential vorticity (PV) equation. A summary

and discussion are given in section 5.

2. Data and method

The synoptic analysis of the plateau vortex in June 2008 is based on the daily precipitation data and the conventional radiosonde data at 12-hour intervals from the China Meteorological Administration. The data used for calculations of the atmospheric apparent heat source and apparent moisture sink, as well as potential vorticity diagnosis, are derived from the final analyses data (FNL) of the Global Forecasting System of the National Centers for Environmental Prediction (NCEP) gridded $1^\circ \times 1^\circ$ at 6-hour intervals (<http://dss.ucar.edu/datasets/ds083.2/>).

A vortex over the Tibetan Plateau is defined as a low occurring over the Tibetan Plateau with closed contour lines or with cyclonic winds at three observation stations at 500 hPa according to the method mentioned by the Lhasa group for Tibetan Plateau meteorology research (1981).

We calculate the atmospheric apparent heat source (Q_1) and the apparent moisture sink (Q_2) based on the thermodynamic equation and the moisture equation, in which the atmospheric heat flux is calculated as the remainder by estimating the large scale components of the local time derivative and horizontal and vertical transports of dry static energy and moisture, respectively. The equations used are as follows (Yanai et al., 1973; Ding, 1989):

$$Q_1 = c_p \left[\frac{\partial T}{\partial t} + \mathbf{V} \cdot \nabla T + \omega \left(\frac{P}{P_0} \right)^\kappa \frac{\partial \theta}{\partial p} \right] \quad (1)$$

$$Q_2 = -L \left(\frac{\partial q}{\partial t} + \mathbf{V} \cdot \nabla q + \omega \frac{\partial q}{\partial p} \right), \quad (2)$$

where T is the temperature, \mathbf{V} and ω denote the horizontal wind component and the vertical wind component in pressure coordinates respectively. P_0 is the pressure of 1000 hPa. c_p represents the specific heat at constant pressure. Its value is $1004 \text{ J Kg}^{-1}\text{K}^{-1}$, and $\kappa \approx 0.286$. θ is the potential temperature. L denotes the latent heat of condensation, and q is the specific humidity. The vertically integrated forms of Eqs. (1) and (2) can be written as follows:

$$\langle Q_1 \rangle \approx LP + S + \langle Q_R \rangle \quad (3)$$

$$\langle Q_2 \rangle \approx LP - LE. \quad (4)$$

Here, $\langle Q_1 \rangle$ and $\langle Q_2 \rangle$ are vertically integrated Q_1 and Q_2 , respectively. P , S , and E represent the amount of precipitation, surface sensible heat flux, and eddy moisture flux, respectively, and $\langle Q_R \rangle$ denotes radiative

heating (cooling).

3. Role of large-scale circulations in the vortex genesis

We chose a vortex over the Tibetan Plateau in the period from 0600 UTC 25 June 2008 to 0000 UTC 26 June 2008 for our analysis. As shown in Fig. 1, the vortex triggered heavy rainfall in the central-eastern plateau, with the rainfall centers located at about (29°N, 96°E) and (30°N, 101°E), respectively.

3.1 500 hPa circulation

Figure 2 presents 500 hPa winds from 0600 UTC 25 June 2008 to 0000 UTC 26 June 2008. At 0600 UTC (Fig. 2a), two lows were located near the Caspian Sea and West Siberia. The huge pressure gradient between the lows and the high over Iran induced strong westerlies to the north of the plateau. Under the influence of the topography of the central-western plateau, one flow turned to be northwesterly and crossed the plateau; the other remained westerly to the north of the plateau. The latter turned to northwesterly wind when it flowed around the northeastern plateau. Meanwhile, there was a cyclone over the Bay of Bengal. The northwesterly wind over the central plateau and the southwesterly wind from the low over the Bay of Bengal formed a trough on the central plateau at about (34°N, 94°E), which was favorable for the formation of the plateau vortex. The cyclonic shear became stronger at 1200 UTC 25 June 2008 (Fig. 2b), and the vortex formed at this time with its center located at (33°N, 97°E). The plateau vortex strength-

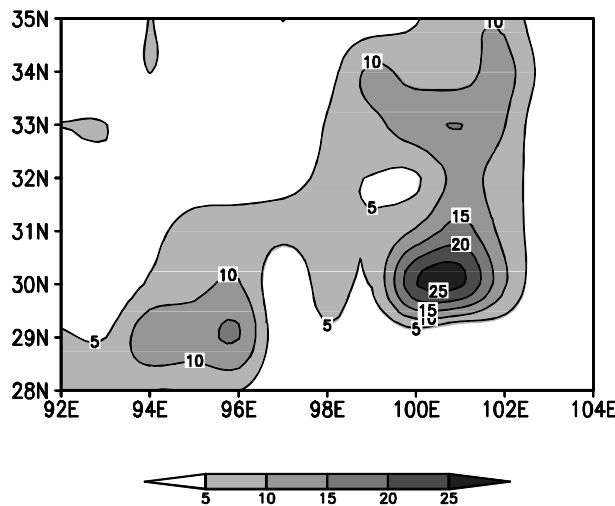


Fig. 1. The observed accumulated rainfall from 1200 UTC 25 June 2008 to 0000 UTC 26 June 2008 (units: mm).

ened from 1200 UTC 25 June 2008 to 1800 UTC 25 June 2008 and moved eastward to (32°N, 100°E) (Fig. 2c). At 0000 UTC 26 June 2008, the vortex reached the sloping terrain at the eastern edge of the Tibetan Plateau with its center located at (32°N, 102°E) (Fig. 2d). The vortex weakened and moved off the plateau with its center located at (33°N, 106°E) at 0600 UTC 26 June 2008, and (32°N, 107°E) at 1200 UTC 26 June 2008 (figure not shown).

Figure 3 shows the 500 hPa winds derived from conventional radiosonde data and the moving track of the vortex. It can be seen that the plateau vortex formed at 1200 UTC 25 June 2008, then moved eastward and persisted for about 30 hours. At 1200 UTC 25 June 2008 (Fig. 3a), there were cyclonic winds centered at (33°N, 95°E), surrounded by Geermu, Naqu, Tuoba, and Yushu meteorological stations. At 0000 UTC 26 June 2008 (Fig. 3b), the center of the cyclonic winds moved to (32°N, 102°E), nearing Dari, Ganzi, and Hongyuan meteorological stations. The vortex reached (32°N, 107°E) and weakened sharply by 1200 UTC 26 June 2008.

From the above analysis, it can be seen that locations of the vortex shown by the winds from conventional radiosonde data are similar to those from FNL data. The difference between them is only 1 to 2 degrees, and their trajectories are almost the same. Therefore, the FNL data is reliable for analyzing this plateau vortex. Considering that the vortex weakened rapidly after moving out of the Tibetan Plateau, we will not discuss the situations after 0600 UTC 26 June 2008.

3.2 200 hPa circulation

Figure 4 shows the geopotential height fields at 200 hPa from 0600 UTC 25 June 2008 to 0000 UTC 26 June 2008. It can be seen that the South Asia High occupied the Tibetan Plateau and intensified gradually from 0600 UTC 25 June 2008 to 1800 UTC 25 June 2008. It began to weaken and retreat westward after 0000 UTC 26 June 2008. In addition, the location of its ridge line was nearly stationary, and the westerlies-northwesterlies to the north of the South Asia High prevailed over the plateau vortex during the whole period.

The 200-hPa jet stream core was located to the northeast of the Tibetan Plateau from 1200 UTC 25 June 2008 to 1800 UTC 25 June 2008, and the divergence area on the right-hand side of the jet was over the vortex. The upper-level divergence at 200 hPa and low-level convergence at 500 hPa were favorable for forming and maintaining the plateau vortex. The intensity of the westerly jet stream became weaker at 0000 UTC 26 June 2008 compared to those at the

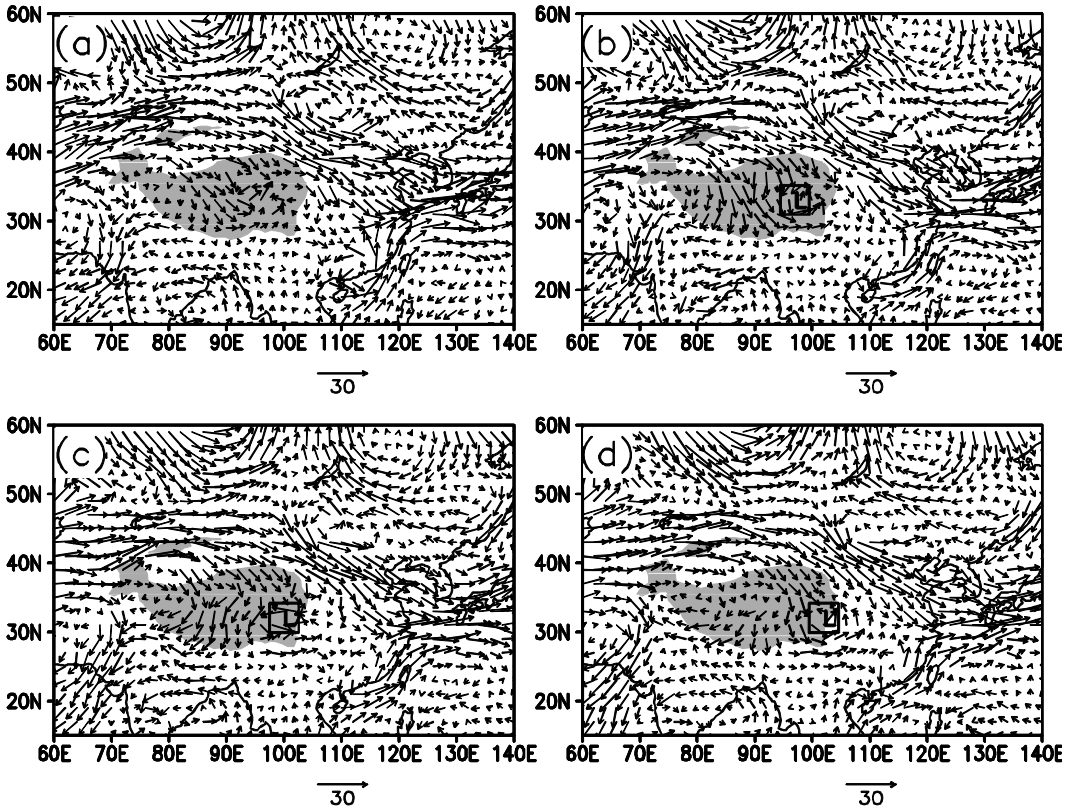


Fig. 2. 500 hPa winds for (a) 0600 UTC 25 June 2008; (b) 1200 UTC 25 June 2008; (c) 1800 UTC 25 June 2008; (d) 0000 UTC 26 June 2008. (Shading indicates the area where topographic height is over 3000 m. “L” indicates the location of the vortex center.)

previous two times. Furthermore, the plateau vortex moved eastward along with the center of the upper jet stream. Yu et al. (2007) pointed out that the strengthening and eastward-stretching of the upper jet stream favored the eastward movement of the plateau vortices, which usually moved under the right-hand side of the westerly jet at 200 hPa. The location of the subtropical westerly jet presented a good indicator for the eastward motion of the plateau vortex.

4. Atmospheric heat source

4.1 *The Atmospheric apparent heat source*

Previous studies indicated that the development of the plateau vortex had a close relationship with the atmospheric heat source over the Tibetan Plateau. In order to investigate how the atmospheric heat source affects the movement of the plateau vortex, firstly, we will analyze the vertical distribution features of the atmospheric apparent heat source.

Figure 5 shows the vertical profiles of Q_1 and Q_2 averaged in the $5^\circ \times 5^\circ$ square area around the vortex center. The absolute value of radiation cooling (Q_R) in Eq. (3) will be far less than that of the condensa-

tion latent heating and the sensible heating when the convection is active. It was rainy during the formation and eastward movement of the vortex, so the influence of Q_R could be ignored.

At 0600 UTC 25 June 2008, during the forming stage of the plateau vortex, the cold northwesterlies over the central plateau converged with the warm and wet southwesterlies from the Bay of Bengal (Fig. 2a), forming a trough and triggering precipitation. From Fig. 5a, it can be seen that the vertical profiles of Q_1 and Q_2 were similar to each other. There was little difference between Q_1 and Q_2 below 500 hPa, indicating that the sensible heat might be very weak at this stage. The maximum of both Q_1 and Q_2 appeared at 400 hPa. Therefore, the latent heat release induced by the precipitation was the major component of the atmospheric heat source at this time (Luo and Yanai, 1984), and it would exert a remarkable effect on the formation of the plateau vortex (Wang, 1987). As a result, the vortex formed at 1200 UTC 25 June 2008. From 1200 UTC 25 June 2008 to 1800 UTC 25 June 2008, under the coaction of the large-scale circulations and the upward motion in the vortex area, the low-level moisture around the vortex center was elevated,

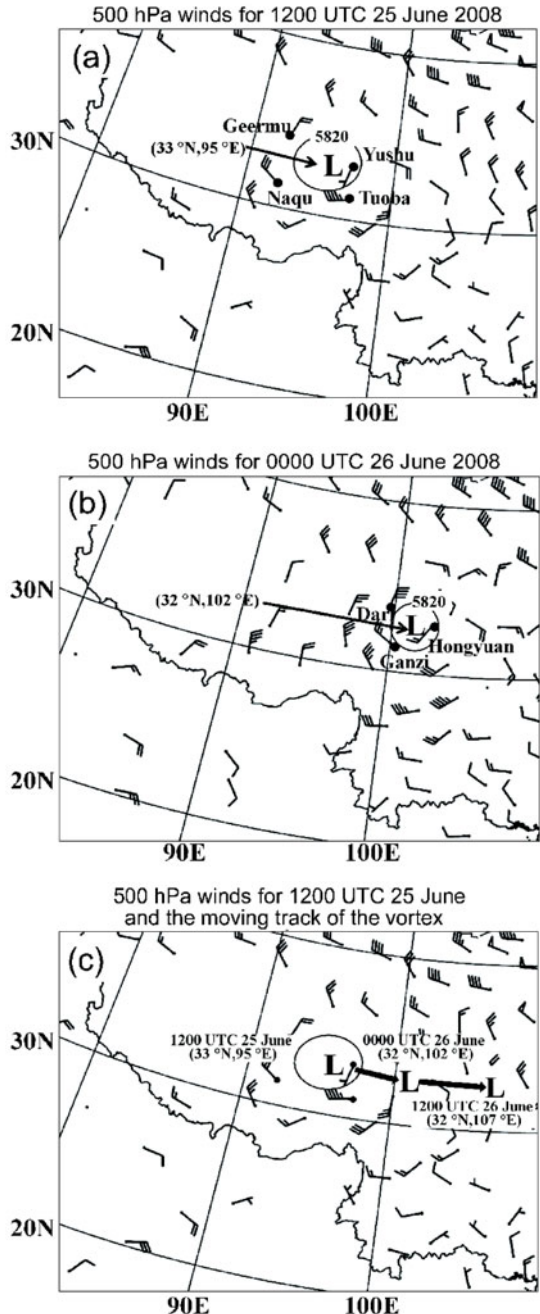


Fig. 3. 500 hPa winds derived from station observations for (a) 1200 UTC 25 June 2008, (b) 0000 UTC 26 June 2008 and (c) the moving track of the vortex [the winds in (c) are for 1200 UTC 25 June 2008]. (“L” indicates the location of the vortex center.)

which was favorable for rainfall. In Figs. 5b and 5c, the height of the maximum Q_2 is lower than that of Q_1 , implying that vertical eddy transport of heat caused by cumulus and turbulence is very important; thus, the atmospheric heating is mainly sourced from the convective rainfall. The corresponding latent heating

would intensify the vortex. At 0000 UTC 26 June 2008, the convergence ascending motion and water vapor transported to the vortex region became weaker compared to those at previous times. Q_1 and Q_2 decreased evidently, with Q_2 smaller than Q_1 , and the height of maximum Q_2 at about 500 hPa with that of Q_1 falling down to 550 hPa. Those features show that the contribution of condensation latent heating decreases remarkably and the sensible heating is the leading part. At this time, the plateau vortex was located in the sloping terrain on the eastern Tibetan Plateau, and its intensity was much weaker than that during the previous 6 hours. How the vertical attribution of the atmospheric heat source affected the movement of plateau vortex will be discussed in the next subsection.

To show the relationship between the atmospheric heat source and eastward movement of the vortex, a time-longitude section of the vertically integrated atmospheric heat source $\langle Q_1 \rangle$ and the vorticity of the vortex is given in Fig. 6. The plateau vortex developed from 1200 UTC 25 June 2008 to 1800 UTC 25 June 2008 and weakened after 0000 UTC 26 June 2008, and its eastward movement was distinctive as well as that of $\langle Q_1 \rangle$. During the eastward-moving period of the vortex, the center of $\langle Q_1 \rangle$ was located to the east of the vortex center. In fact, the southwesterly wind from the southeastern side of the vortex and the northwesterly wind over the northeastern plateau converged to the east of the vortex center (see Fig. 2). The convergence likely caused upward motion and condensation latent heating accordingly. Therefore, the heating center appeared to the east of the vortex center.

4.2 The effect of the atmospheric heat source on the intensity and movement of the plateau vortices

In order to understand the role the atmospheric heat source played in the mechanism of eastward motion and the development of the plateau vortex, the Ertel PV equation (Wu, 2001) is utilized to analyze the potential vorticity budget. The PV tendency equation without the friction effect can be given as follows:

$$\frac{dP_E}{dt} = \alpha \zeta_a \cdot \nabla Q, \quad (5)$$

where P_E represents Ertel PV, α is the specific volume, and $\zeta_a = (f\mathbf{k} + \nabla_3 \times \mathbf{V})$ is the absolute vorticity, \mathbf{k} and \mathbf{V} denote the unit vector in Z direction and wind vector, respectively. Q is the diabatic heating rate. The PV in pressure coordinates is

$$P_E = -g(f + \zeta_p) \frac{\partial \theta}{\partial p} + g \left(\frac{\partial v}{\partial p} \frac{\partial \theta}{\partial x} - \frac{\partial u}{\partial p} \frac{\partial \theta}{\partial y} \right), \quad (6)$$

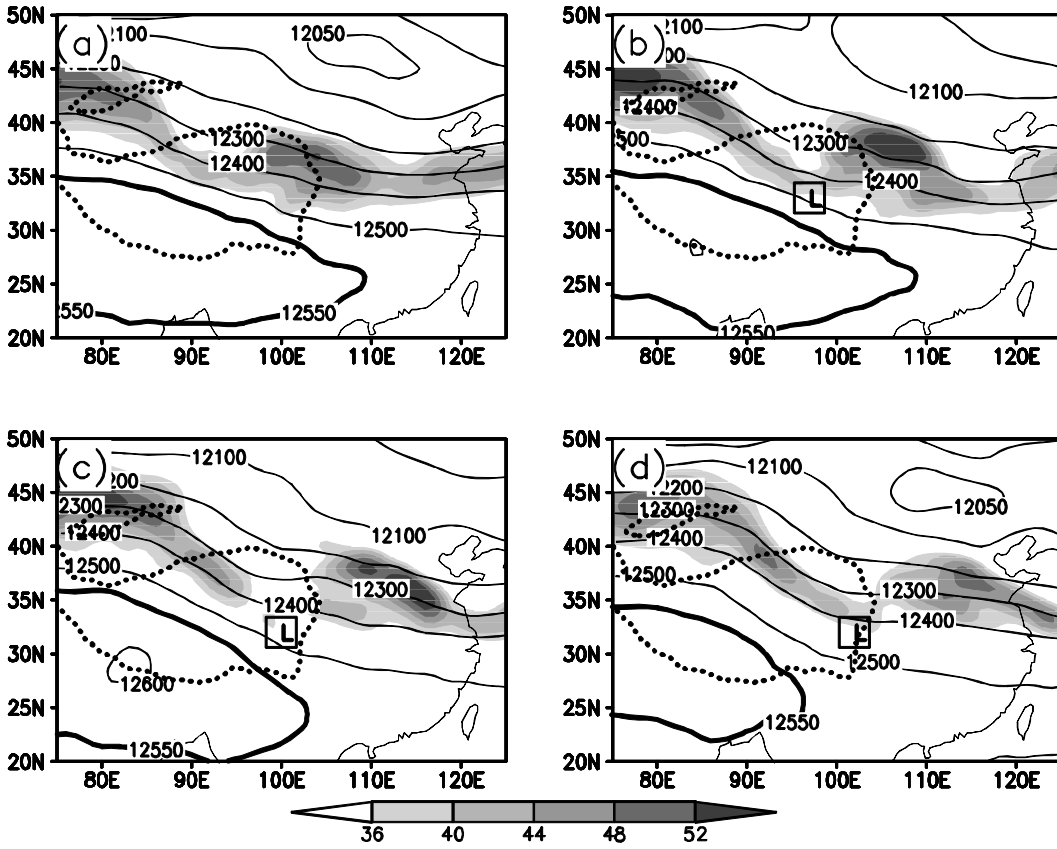


Fig. 4. 200 hPa geopotential height (solid line, units: gpm) and wind speed (shadings, units: m s^{-1}) for (a) 0600 UTC 25 June 2008, (b) 1200 UTC 25 June 2008, (c) 1800 UTC 25 June 2008, (d) 0000 UTC 26 June 2008. (“L” indicates the location of the vortex center at 500 hPa. Area enclosed by 12550 gpm denotes South Asia High. The dotted lines are the topographic contours of 3000 m.)

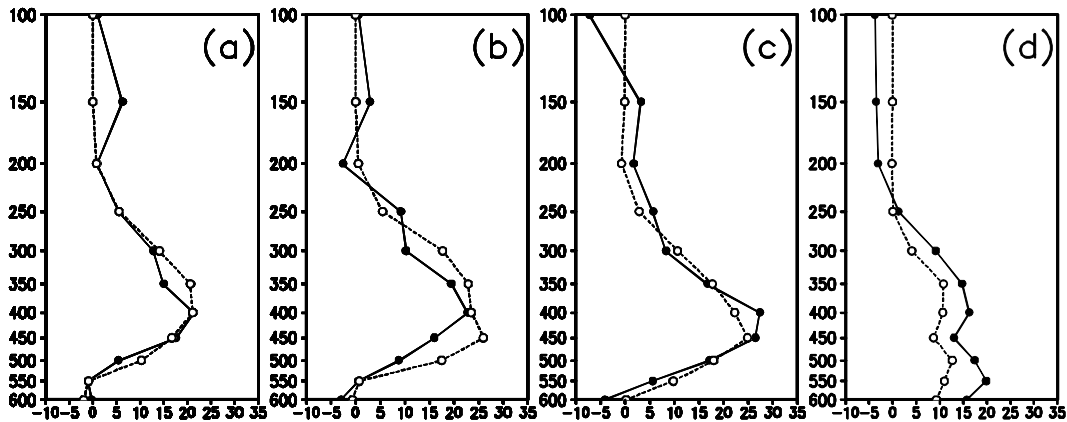


Fig. 5. Vertical profiles of the atmospheric heat source (Q_1) (solid line, units: K d^{-1}) and atmospheric moist sink (Q_2) (dashed line, units: K d^{-1}) averaged in the $5^\circ \times 5^\circ$ square area around the vortex center for (a) 0600 UTC 25 June 2008, (b) 1200 UTC 25 June 2008, (c) 1800 UTC 25 June 2008, (d) 0000 UTC 26 June 2008.

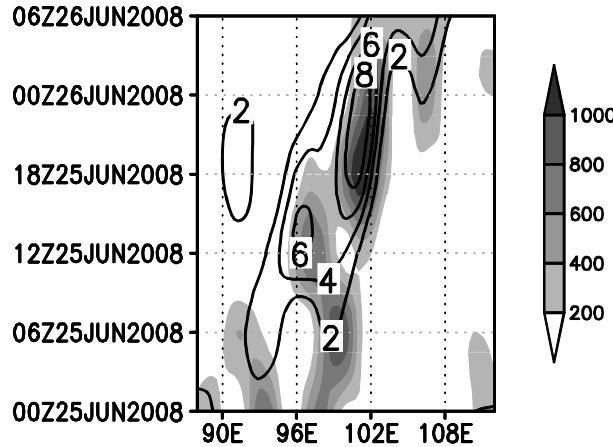


Fig. 6. Time-longitude section of vertically integrated atmospheric heat source ($\langle Q \rangle$) (shadings, units: W m^{-2}) and 500 hPa vertical vorticity averaged between 30°N and 33°N (isolines, units: 10^{-5} s^{-1}).

where θ is the potential temperature, f denotes the geostrophic vorticity, and u and v represent zonal and meridional wind respectively. The right-hand side of Eq. (5) can be written as

$$\alpha \zeta_a \cdot \nabla Q = \alpha \left[\zeta_x \frac{\partial Q}{\partial x} + \zeta_y \frac{\partial Q}{\partial y} + (f + \zeta_z) \frac{\partial Q}{\partial z} \right], \quad (7)$$

where ζ_x , ζ_y , and ζ_z denote the zonal, meridional, and vertical vorticity, respectively. Because $\partial w / \partial y$ and $\partial w / \partial x$ are far less than $\partial v / \partial z$ and $\partial u / \partial z$, we make approximate transformations as follows (Wu et al., 1999; Liu et al., 2001)

$$\begin{cases} \zeta_x = \frac{\partial w}{\partial y} - \frac{\partial v}{\partial z} \approx -\frac{\partial v}{\partial z} & \xrightarrow{\text{coordinate transformation}} \rho g \frac{\partial v}{\partial p} \\ \zeta_y = \frac{\partial u}{\partial z} - \frac{\partial w}{\partial x} \approx \frac{\partial u}{\partial z} & \xrightarrow{\text{coordinate transformation}} -\rho g \frac{\partial u}{\partial p} \\ \zeta_z = \zeta_p = \frac{\partial v}{\partial x} - \frac{\partial u}{\partial y}. \end{cases} \quad (8)$$

Thus, we can get

$$\alpha \zeta_a \cdot \nabla Q \approx g \left[\frac{\partial v}{\partial p} \frac{\partial Q}{\partial x} - \frac{\partial u}{\partial p} \frac{\partial Q}{\partial y} - (f + \zeta_p) \frac{\partial Q}{\partial p} \right], \quad (9)$$

where ζ_p is the vertical vorticity in pressure coordinates. Therefore, Eq. (5) can be expanded as

$$\begin{aligned} \frac{\partial P_E}{\partial t} = & -\frac{\partial u P_E}{\partial x} - \frac{\partial v P_E}{\partial y} - \frac{\partial \omega P_E}{\partial p} + \\ & g \frac{\partial v}{\partial p} \frac{\partial Q}{\partial x} - g \frac{\partial u}{\partial p} \frac{\partial Q}{\partial y} - g(f + \zeta_p) \frac{\partial Q}{\partial p}. \end{aligned} \quad (10)$$

The first two terms on the right-hand side of Eq. (10) are the horizontal PV flux divergence. The third term is the vertical PV flux divergence. The fourth and the

fifth terms are related to redistribution of PV induced by the horizontally uneven distribution of Q , and the sixth term arises from the vertically uneven distribution of Q . Equation (10) indicates that contributions to the local PV change arise from the horizontal and vertical PV flux divergence and the PV redistribution due to the spatially uneven distribution of Q (Pan et al., 2008). In our calculation, we take Q_1 as Q to discuss the effect of latent heating on the intensity and moving direction of the vortex.

Because the PV budgets from 0600 UTC to 1800 UTC 25 June 2008 are similar, we analyzed the PV budgets during this period by using the dynamic composite method. This method was used to study typhoons by Li et al. (2005) and Ren et al. (2008). The so-called “dynamic composite method” is to take the vortex center as the origin of coordinates which moves with the vortex and limit the same scope at each time, then make a composite in the moving coordinate system for each time. Here, the convergence center on the stream field was defined as the center of the vortex at each time. We made the PV budget composite at different times with the vortex centers coinciding with each other. The schematic diagram is given in Fig. 7. The composite of 500 hPa PV budgets is shown in Fig. 8.

Before 0000 UTC 26 June 2008, when the vortex intensity began to decrease, the vortex center coincided with the positive contribution center of the horizontal PV flux convergence (Fig. 8a). The negative contribution center of the vertical PV flux divergence was located to the east of the vortex center (Fig. 8b), where Q_1 had a positive effect on the PV tendency (Fig. 8c). To highlight the total net contributions to the PV tendency from the horizontal PV flux divergence, vertical PV flux diver-

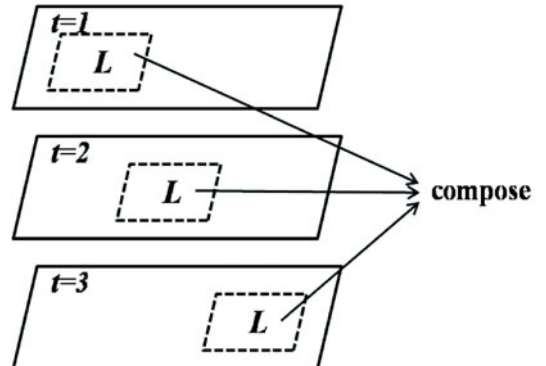


Fig. 7. Schematic diagram of Dynamic Composite Analysis Method. (The square areas enclosed by solid line indicate the background field at 500 hPa, and those enclosed by dashed line present the regions centering on the vortex's center. “L” indicates the location of the vortex center.)

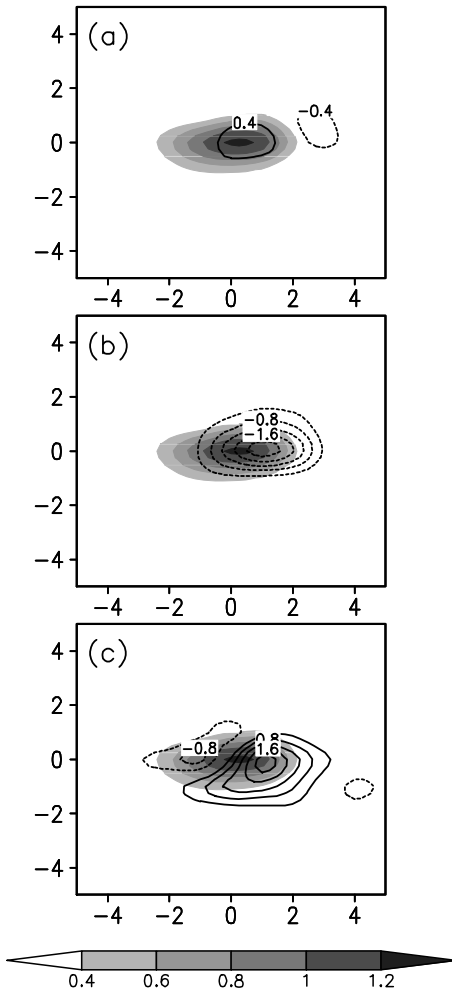


Fig. 8. Composite of 500 hPa PV (shadings, units: PVU, $1\text{PVU} = 10^{-6} \text{ K m}^2 \text{ s}^{-1} \text{ kg}^{-1}$), (a) the horizontal PV flux divergence, (b) the vertical PV flux divergence and (c) PV tendency induced by apparent heat source (isolines, units: PVU (6 h) $^{-1}$, $1\text{PVU} = 10^{-6} \text{ K m}^2 \text{ s}^{-1} \text{ kg}^{-1}$) at 0600 UTC, 1200 UTC and 1800 UTC 25 June 2008. The origin of coordinates is the vortex center. Coordinate units are 1° latitude (longitude).

gence, and apparent heat source, their averages are shown in Fig. 9 for 0600 UTC, 1200 UTC and 1800 UTC 25 June 2008, respectively. The figure shows that although the positive contribution from the heat source was partly cancelled by the negative contribution from the vertical PV flux, there was still a net positive effect to the east and southeast of the vortex. In fact, from Figs. 2 and 3, we can see that while the vortex moves eastward, it also moves southward slightly. Thus, the prominent factor which attributed to the eastward movement of the vortex is not the horizontal or vertical PV flux divergence but Q_1 , which induced a positive PV tendency to the east of the vortex center and was helpful to the development and

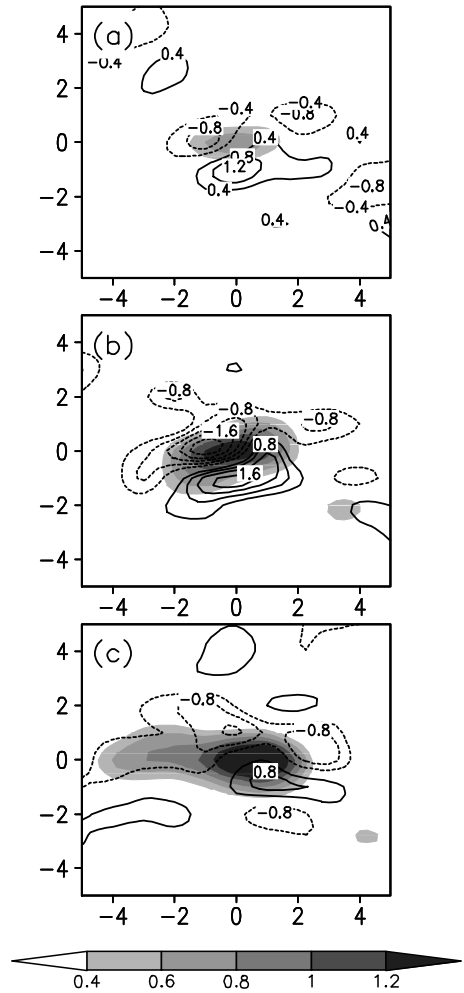


Fig. 9. Total net effects of horizontal PV flux divergence, vertical PV flux divergence and apparent heat source at (a) 0600 UTC 25 June 2008, (b) 1200 UTC 25 June 2008 and (c) 1800 UTC 25 June 2008 (isolines, units: PVU (6 h) $^{-1}$, $1\text{PVU} = 10^{-6} \text{ K m}^2 \text{ s}^{-1} \text{ kg}^{-1}$). Shadings are 500 hPa PV (units: PVU). The origin of coordinates is the vortex center. Coordinate units are 1° latitude (longitude).

eastward movement of the vortex.

At 0000 UTC 26 June 2008, the effect of Q_1 at 500 hPa was almost negative around the vortex center (Fig. 10c), which weakened the vortex. Meanwhile, there was a positive PV tendency caused by the horizontal PV flux convergence to the east of the vortex. As a result, their joint effects made the vortex move eastward and weaken.

Since Q_1 might be a major factor affecting the movement of the plateau vortex, we illustrate the time-longitude section of the total contribution of Q_1 to the local variation of PV [last three terms of Eq. (10)] and the vertical vorticity together (Fig. 11).

During the developing stage of the vortex from

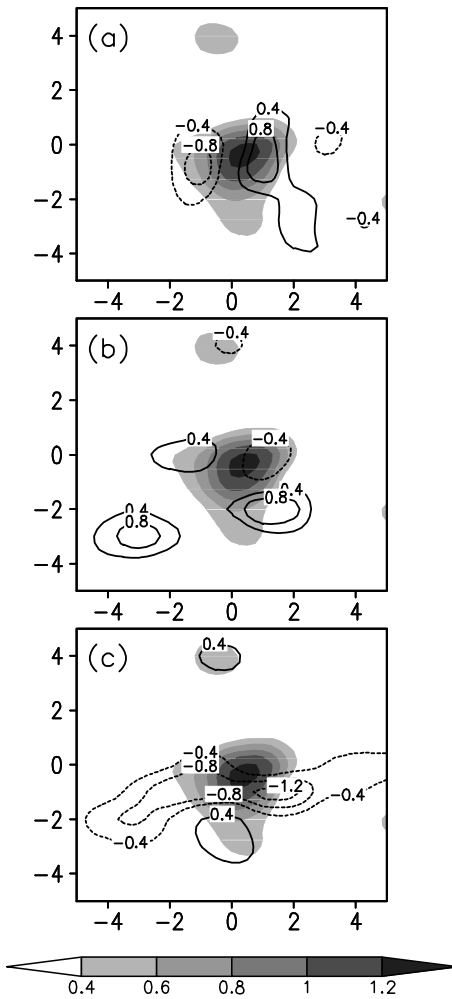


Fig. 10. 500-hPa PV (shadings, units: PVU, $1\text{PVU} = 10^{-6} \text{ K m}^2 \text{ s}^{-1} \text{ kg}^{-1}$), (a) the horizontal PV flux divergence, (b) the vertical PV flux divergence and (c) PV tendency induced by apparent heat source at 0000 UTC 26 June 2008 (isolines, units: $1\text{PVU} (6 \text{ h})^{-1}$, $1\text{PVU} = 10^{-6} \text{ K m}^2 \text{ s}^{-1} \text{ kg}^{-1}$). The origin of coordinates is the vortex center. Coordinate units are 1° latitude (longitude).

1200 UTC 25 June 2008 to 1800 UTC 25 June 2008, the positive contribution centers of Q_1 were located in the vortex center and to its east, which was favorable for strengthening and eastward moving of the vortex as we discussed above. At 0000 UTC 26 June 2008, the effect of Q_1 was almost negative around the vortex center. Correspondingly, the vortex began to weaken.

In order to illustrate how the atmospheric heat source affected the intensity and trajectory of the vortex, we show in Fig. 12 the effect of the horizontal distribution of $Q_1 \left(g \frac{\partial v}{\partial p} \frac{\partial Q_1}{\partial x} - g \frac{\partial u}{\partial p} \frac{\partial Q_1}{\partial y} \right)$ and that of the vertical distribution of $Q_1 \left(-g(f + \zeta_p) \frac{\partial Q_1}{\partial p} \right)$ on PV tendency, respectively.

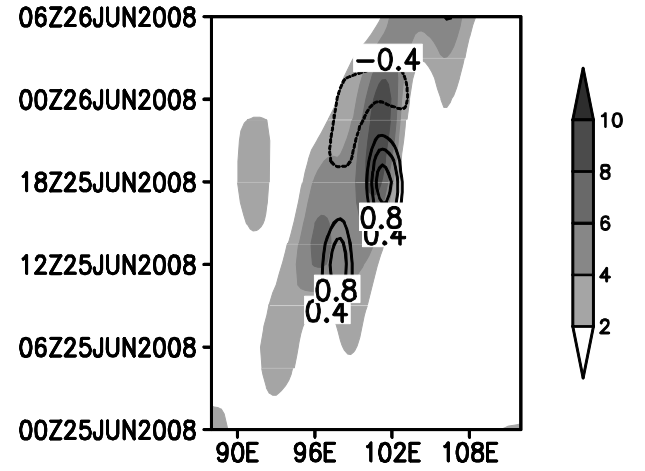


Fig. 11. Time-longitude section of the vertical vorticity (shadings, units: 10^{-5} s^{-1}) and contribution of atmospheric heat source to the local PV [isolines, units: $1\text{PVU} (6 \text{ h})^{-1}$, $1\text{PVU} = 10^{-6} \text{ K m}^2 \text{ s}^{-1} \text{ kg}^{-1}$] averaged between 30° – 33°N .

From 1200 UTC 25 to 1800 UTC 25 June 2008, the vertical term (Figs. 12b and d) was remarkably greater than the horizontal term (Figs. 12a and c). Obviously, the effect of the vertical distribution of Q_1 was much more prominent. Such a feature can be explained as follows. When the water vapor converged and ascended at 400 hPa–450 hPa, the latent heat was released and the upper atmosphere was heated. Upper-level heating ($-\frac{\partial Q_1}{\partial p} > 0$) depressed the lower isobaric surface and strengthened the low-level cyclonic circulation (Wu et al., 2008, 2009). Consequently, the vortex strengthened when the upper-level heating center coincided with the vortex center. Meanwhile, since the convergent ascending motion was to the east of the vortex, there was a negative effect of the vertical PV flux divergence center and a weak positive effect of the horizontal PV flux convergence center around the vortex center (see Figs. 8a and b). Their coaction forced a positive PV net budget to the east of the vortex center, which was helpful to its eastward movement.

At 0000 UTC 26 June 2008 (Figs. 12e and f), although the vertical distribution effect of Q_1 was still positive to the east of the vortex, it was far less than the negative effect caused by the horizontally uneven distribution of Q_1 . The horizontal distribution effect became prominent, which was not in favor of the eastward motion and decreased the intensity of the vortex. The calculation results indicate that Q_1 on the east of the vortex became weaker and that on the south of the vortex was relatively stronger. Under this spatial distribution of Q_1 , the horizontal vortex tube ($\zeta_y = -\rho g \frac{\partial u}{\partial p} > 0$) around the vortex center was forced to slant because the Q_1 center was to the south

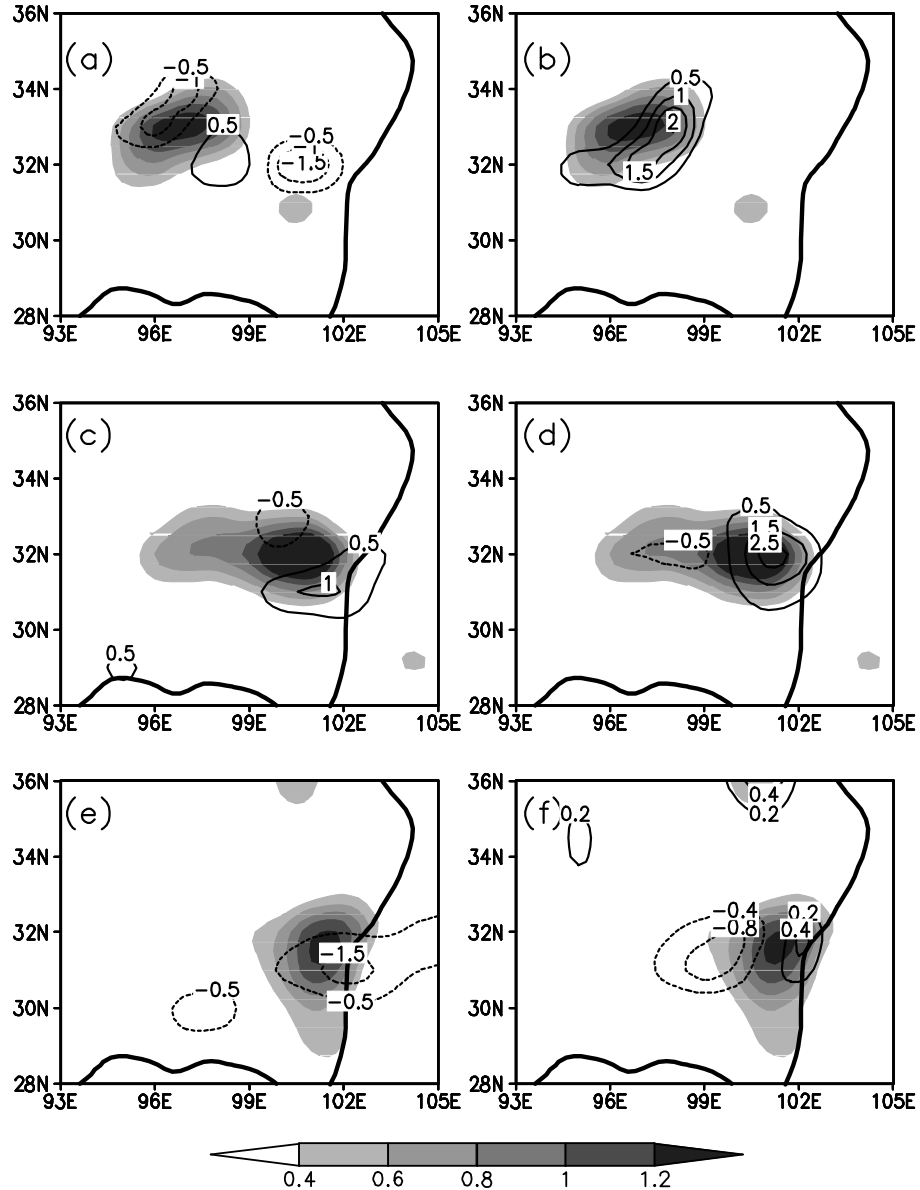


Fig. 12. 500 hPa PV (shadings, units: PVU, $1\text{PVU} = 10^{-6} \text{ K m}^2 \text{ s}^{-1} \text{ kg}^{-1}$), contributions from the horizontal (left panel: a, c, e) and the vertical (right panel: b, d, f) distributions of the atmospheric heat source (isolines, units: $1\text{PVU} (6 \text{ h})^{-1}$, $1\text{PVU} = 10^{-6} \text{ K m}^2 \text{ s}^{-1} \text{ kg}^{-1}$). (a) and (b) for 1200 UTC 25 June 2008, (c) and (d) for 1800 UTC 25 June 2008, (e) and (f) for 0000 UTC 26 June 2008. (Thick solid lines are the topographic contours of 3000 m.)

of the vortex at 500 hPa ($\frac{\partial Q_1}{\partial y} < 0$), leading to the negative vertical vorticity component which weakened the vortex intensity ($-g \frac{\partial u}{\partial p} \frac{\partial Q_1}{\partial y} < 0$). In addition, to the east of the vortex, the effect of the horizontal PV flux divergence was positive, resulting in the vortex turning to move eastward with its intensity decreasing.

5. Summary and concluding remarks

In this paper we investigate mechanisms of the formation, development, and eastward motion for a low-level cyclonic vortex over the main body of the Tibetan Plateau in June 2008. When the vortex was over the Tibetan Plateau, the lows located near the Caspian Sea and West Siberia, the high over Iran, and the Bay of Bengal low were the major synoptic systems at 500

hPa. In the formation stage of the vortex, a strong northwesterly invaded the central Tibetan Plateau and converged with the southerly induced by the Bay of Bengal low. In addition, the convergence area at 500 hPa was located just below the entrance region of the upper westerly jet at 200 hPa. The upper-level divergence and low-level convergence, as well as the latent heat release caused by convergent ascending motion, were favorable for the formation of the plateau vortex.

The atmospheric heat source played an important role in the development and movement of the vortex. In its eastward-moving process, the center of the vertically integrated atmospheric heat source ($\langle Q_1 \rangle$) was always located to the east of the vortex center because of the convergence of southwesterlies and northwestwesterlies. The dynamical diagnosis of the PV equation shows that vertically uneven distribution of the heating will give rise to a positive PV tendency to the east of the vortex and make the vortex shift eastward. Therefore, the vertically uneven distribution of the atmospheric heat source (Q_1) played an important role in the eastward movement of the vortex and in its increased intensity when the heating center over 500 hPa coincided with the vortex center at 500 hPa. The horizontally uneven distribution of Q_1 became prominent when the vortex began to weaken. The uneven heating caused horizontal vortex tube slants at 500 hPa and affected the intensity and moving direction of the vortex through the vertical vorticity component of the slanted vortex tube. The intensity and moving direction of the vortex depended on both the vorticity fields and the spatial distribution of the atmospheric heat source.

It should be pointed out that our diagnosis results are only for one case. The study of more cases is still needed to further understanding of the mechanisms of the plateau vortex. The plateau vortices are unique products over the Tibetan Plateau, the dynamic forcing of the plateau provides a favorable circulation background for the latent heat release to take place. The northwesterly wind over the central plateau and the northeastern plateau we mentioned in this paper may all have a close relationship with the topography of Tibetan Plateau, which has a dominant role in the development process (Shen et al., 1986a; Dell'Osso and Chen, 1986; Wang, 1987). The concrete influence of the topography should be further investigated through numerical experiment. In addition, the vortex origin is still an open question. For example, some researches pointed out that the released condensation latent heat was favorable for the genesis of the vortex (Dell'Osso and Chen, 1986; Wang, 1987), while others stressed the role of the sensible heating (Lhasa group for Tibetan Plateau meteorology research, 1981; Shen et al., 1986b; Li and Zhao, 2002). Our results

provide a clue that the vortex genesis may be associated with the convergence between westerlies from the north and southerlies from the Bay of Bengal. Additional detailed diagnostic analyses are needed to look into the mechanism of the vortex genesis.

Acknowledgements. The authors are very grateful to Dr. C.-H. Sui and two anonymous reviewers for their constructive comments, to the information center of Chinese Academy of Meteorological Sciences for providing the observational data, and also to Dr. PAN Yang for suggestions which improved the calculation programs. This work was supported by the National Natural Science Foundation of China (Grant No. 40921003), the National Key Program for Developing Basic Sciences (Grant No. 2004CB418300), and the International S&T Cooperation Project of the Ministry of Science and Technology of China under Grant No. 2009DFA21430.

REFERENCES

- Chen, B. M., Z. A. Qian, and L. S. Zhang, 1996: Numerical simulation of formation and development of vortices over the Qinghai-Xizang Plateau in summer. *Chinese J. Atmos. Sci.*, **20**, 491–502. (in Chinese)
- Dell'Osso, L., and S. J. Chen, 1986: Numerical experiments on the genesis of vortices over the Qinghai-Xizang Plateau. *Tellus*, **38**(A), 235–250.
- Ding, Y. H., 1989: *The Diagnostic Analysis Methods of Synoptic Dynamics*. Science Press, Beijing, 293pp. (in Chinese)
- Ding, Z. Y., and J. N. Lu, 1990: A numerical experiment on the eastward movement of a Qinghai-Xizang Plateau low vortex. *Journal of Nanjing Institute of Meteorology*, **13**, 426–431. (in Chinese)
- Lhasa group for Tibetan Plateau meteorology research, 1981: *Research of 500 hPa Shear Lines over the Tibetan Plateau in Summer*. Science Press, Beijing, 122pp. (in Chinese)
- Li, G. P., 2002: *The Tibetan Plateau Dynamic Meteorology*. China Meteorological Press, Beijing, 271pp. (in Chinese)
- Li, G. P., and B. J. Zhao, 2002: A dynamical study of the role of surface sensible heating in the structure and intensification of the Tibetan Plateau vortices. *Chinese J. Atmos. Sci.*, **26**, 519–525. (in Chinese)
- Li, G. P., and H. W. Liu, 2006: A dynamical study of the role of surface heating on the Tibetan Plateau vortices. *Journal of Tropical Meteorology*, **22**, 632–637. (in Chinese)
- Li, Y., L. S. Chen, and J. Z. Wang, 2005: Diagnostic study of the sustaining and decaying of tropical cyclones after landfall. *Chinese J. Atmos. Sci.*, **29**, 482–490. (in Chinese)
- Liu, F. M., and M. J. Fu, 1985: A study on the moving eastward Lows over Qinghai-Xizang Plateau. *Plateau Meteorology*, **5**, 125–134. (in Chinese)

- Liu, Y. M., G. X. Wu, H. Liu, and P. Liu, 2001: Dynamical effects of condensation heating on the subtropical anticyclones in the Eastern Hemisphere. *Climate Dyn.*, **17**, 327–338.
- Luo, H. B., and M. Yanai, 1984: The large-scale circulation and heat sources over the Tibetan Plateau and surrounding areas during the early summer of 1979. Part II: Heat and moisture budgets. *Mon. Wea. Rev.*, **112**, 966–989.
- Luo, S. W., 1992: *Study on Some Kinds of Weather Systems over and around the Qinghai-Xizang Plateau*. China Meteorological Press, Beijing, 205pp. (in Chinese)
- Luo, S. W., Y. Yang, and S. H. Lu, 1991: Diagnostic analyses of a summer vortex over Qinghai-Xizang Plateau for 29–30 June 1979. *Plateau Meteorology*, **10**, 1–11. (in Chinese)
- Luo, S. W., M. L. He, and X. D. Liu, 1993: Study on summer vortices over Qinghai-Xizang Plateau. *Science in China (B)*, **23**, 778–784. (in Chinese)
- Pan, Y., R. C. Yu, J. Li, and Y. P. Xu, 2008: A case study on the role of water vapor from southwest China in downstream heavy rainfall. *Adv. Atmos. Sci.*, **25**(3), 563–576, doi: 10.1007/s00376-008-0563-x.
- Qiao, Q. M., 1987: The environment analysis on 500hPa vortexes moving eastward out of Tibet Plateau in summer. *Plateau Meteorology*, **6**, 45–54. (in Chinese)
- Qiao, Q. M., and Y. G. Zhang, 1994: *Synoptic Meteorology of the Tibetan Plateau*. China Meteorological Press, Beijing, 251pp. (in Chinese)
- Ren, S. L., Y. M. Liu, and G. X. Wu, 2008: Interaction between typhoon and western Pacific subtropical anticyclone: data analyses and numerical experiments. *Acta Meteorologica Sinica*, **22**, 329–341.
- Shen, R. J., E. R. Reiter, and J. F. Bresch, 1986a: Numerical simulation of the development of vortices over the Qinghai-Xizang (Tibet) Plateau. *Meteor. Atmos. Phys.*, **35**, 70–95.
- Shen, R. J., E. R. Reiter, and J. F. Bresch, 1986b: Some aspects of the effects of sensible heating on the development of summer weather system over the Qinghai-Xizang Plateau. *J. Atmos. Sci.*, **43**, 2241–2260.
- Wang, B., 1987: The development mechanism for Tibetan Plateau warm vortices. *J. Atmos. Sci.*, **44**, 2978–2994.
- Wu, G. X., 2001: Comparison between the complete-form vorticity equation and the traditional vorticity equation. *Acta Meteorologica Sinica*, **59**, 386–392. (in Chinese)
- Wu, G. X., Y. M. Liu, and P. Liu, 1999: Spatially inhomogeneous diabatic heating and its impacts on the formation and variation of subtropical anticyclone, I. Scale analysis. *Acta Meteorologica Sinica*, **57**, 257–263. (in Chinese)
- Wu, G. X., Y. M. Liu, J. J. Yu, X. Y. Zhu, and R. C. Ren, 2008: Modulation of land-sea distribution on air-sea interaction and formation of subtropical anticyclones. *Chinese J. Atmos. Sci.*, **32**, 720–740. (in Chinese)
- Wu, G. X., Y. Liu, X. Zhu, W. Li, R. Ren, A. Duan, and X. Liang, 2009: Multi-scale forcing and the formation of subtropical desert and monsoon. *Ann. Geophys.*, **27**, 3631–3644.
- Yanai, M., E. Steven, and J. H. Chu, 1973: Determination of bulk properties of tropical cloud clusters from large-scale heat and moisture budgets. *J. Atmos. Sci.*, **30**, 611–627.
- Ye, D. Z., and Y. X. Gao, 1979: *The Tibetan Plateau Meteorology*. Science Press, Beijing, 278pp. (in Chinese)
- Yu, S. H., W. L. Gao, and Q. Y. Gu, 2007: The middle-upper circulation analyses of the Plateau low vortex moving out of Plateau and influencing flood in east China in recent years. *Plateau Meteorology*, **26**, 466–475. (in Chinese)